

Mapping snow cover and snow depth across the Lake Limnopolar watershed on Byers Peninsula, Livingston Island, Maritime Antarctica

S.R. FASSNACHT¹, J.I. LÓPEZ-MORENO², M. TORO³ and D.M. HULTSTRAND¹

¹ESS-Watershed Science, Colorado State University, Fort Collins, CO 80523-1476, USA

²Instituto Pirenaico de Ecología, CSIC, Zaragoza, Spain

³Área de Medio Ambiente Hídrico, Centro de Estudios Hidrográficos (CEDEX), Madrid, Spain
Steven.Fassnacht@colostate.edu

Abstract: Few parts of Antarctica are not permanently covered in ice. The retreat of the ice sheet from Byers Peninsula on western Livingston Island, Maritime Antarctica, has provided a new area of seasonal snow cover. Snow surveys were conducted in late November 2008 at the time of peak accumulation across the 1 km² Lake Limnopolar watershed. Topographic variables were derived from a digital elevation model to determine the variables controlling the presence or absence of snow and the distribution of snow depth. Classification with binary regression trees showed that wind related variables dominated the presence and depth of snow. The product of the sine of aspect and the sine of slope was the first variable in both regression trees. Density profiles were also measured and illustrated a relatively homogeneous snowpack over space at peak snow accumulation.

Received 31 January 2012, accepted 1 October 2012

Key words: binary regression trees, density, South Shetland Islands, topographic drivers

Introduction

Snow is a dominant feature on the Antarctic landscape. While most of Antarctica is covered by permanent ice, small coastal areas do become snow-free during the summer months. In the future, these could be expanded by a warming climate, such as has been observed in areas of West Antarctica (Anisimov *et al.* 2007). Byers Peninsula on Livingston Island, South Shetland Islands, is one of the largest ice-free areas of Maritime Antarctica (Thomson & López-Martínez 1996). In this region, annual precipitation is higher than on continental Antarctica (Van Lipzig *et al.* 2004), and typically ranges from 700–1000 mm (Bañón 2004).

Snow is a dynamic medium that changes continuously and forcing processes operate at multiple scales. Small research areas studied in detail may exhibit extreme heterogeneity, while larger research areas studied in less detail may exhibit patterns and homogeneity (Blöschl 1999). For Antarctica, a limited number of studies have examined the spatial distribution of snow and most have focused on continental Antarctica, such as Dronning Maud Land (e.g. Richardson-Näslund 2004, Vihma *et al.* 2011). Station meteorological data have been collected along the Antarctica Peninsula and used to determined snowpack sublimation and drift in regional atmospheric models (e.g. Van Lipzig *et al.* 2004) or in Maritime Antarctica for energy balance studies of the King George Island ice cap (e.g. Bintanja 1995, Braun & Hock 2004).

To date, no data have been published on the distribution of snow in Maritime Antarctica. In this study snowpack

data were collected on Byers Peninsula in late November 2008 as part of a Spanish Polar Commission contribution to the International Polar Year. This paper presents the distribution of snow depth and since the variation of snow density is often assumed to be limited across a watershed (Elder *et al.* 1991), the density variation down the snowpack will be presented for five different locations.

The distribution of snow

Much of the research examining the distribution of snow has focused on mountainous regions. Meiman (1968) presented the correlation between snow accumulation patterns and topographic variables (elevation and aspect) as well as forest canopy properties. Subsequent research has used topographic variables as surrogates for the meteorological variables that dictate the distribution of snow in alpine regions (Elder *et al.* 1991, Winstral *et al.* 2002). Various methods have been used to relate topography with the distribution of snow, such as binary regression trees (Elder *et al.* 1991) and geostatistics (Erxleben *et al.* 2002). A comparison of interpolation methods often illustrates that the optimal method is location specific (Erxleben *et al.* 2002, López-Moreno & Nogués-Bravo 2006).

Snow sampling has occurred at several location across the Arctic. The distribution of snow has been investigated in areas such as the Canadian Archipelago (e.g. Woo 1998) and Svalbard (e.g. Bruland *et al.* 2001, Winther *et al.* 2003). The work in the Canadian high Arctic focused on

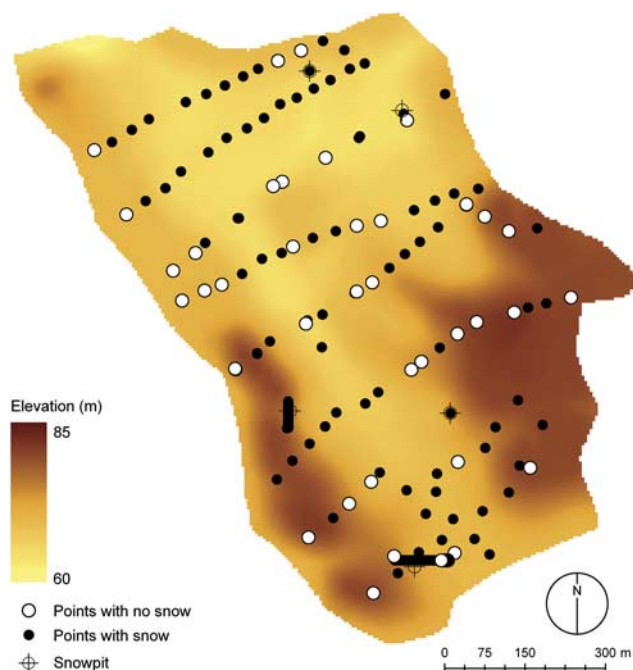


Fig. 1. The distribution of elevation and the location of the snow depth measurements (snow-covered and snow-free) and the snow pits.

watersheds of about the same size as the Byers basin, while much of the Svalbard work focused on larger areas where elevational gradients dictate accumulation amounts (Winther *et al.* 2003). An important difference between the Arctic regions and this study site is that the Arctic sites are located closer to the pole and receive substantially less solar radiation with no sunlight for several months during the winter. The Canadian sites are also much drier with only a fraction of the annual precipitation (100–200 mm vs 700–1000 mm) typical for Byers Peninsula. The present study considered the influence of solar radiation, which can be important for metamorphism during accumulation and specifically for ablation.

Very limited vegetation is present in Maritime Antarctica. With the absence of trees and shrubs, strong winds can play a significant role in snow distribution through sublimation, wind scour and deposition (Essery *et al.* 1999, Winstral & Marks 2002, Erickson *et al.* 2005). For less rugged terrain with limited large vegetation, such as the Canadian prairies, slope and curvature have been shown to influence local meteorological conditions that drive the distribution of snow (Lapen & Martz 1996).

Since the Byers Peninsula may be different from alpine or prairie regions where the distribution of snow has been examined, the objectives for this paper are: 1) to determine the topographic variables controlling the presence (snow-covered) or absence (snow-free) of snow, and 2) to determine the topographic variables controlling the distribution of snow depth (within the snow-covered area).

Study site

The Lake Limnopolar basin is a small tundra watershed (Fig. 1) located at *c.* 62°40'S, 60°5'W on Byers Peninsula on the west side of Livingston Island, South Shetland Islands, Antarctica (Quesada *et al.* 2009). Byers Peninsula is of interest for climate change research since it started deglaciating in the last 5000 years with the most recent retreats occurring *c.* 400 years ago (Björck *et al.* 1996). The western terminus of the Rotch Dome ice cap that covers Livingston Island is 6.5 km to the east of the watershed.

Livingston Island has a much less extreme climate than continental Antarctica. Mean summer temperatures range from 1–3°C with daily maximums and minimums being $\pm 10^\circ\text{C}$ (Rochera *et al.* 2010). Winter temperatures remain colder than 0°C with lows reaching -27°C (Rochera *et al.* 2010). The region is snow-covered for eight or more months of the year with some perennial snowpacks. Winds blow mostly from the west with average speeds from 5–15 m s⁻¹ during peak accumulation (Fassnacht *et al.* 2010).

Methods

Snow data

Snow depths were measured across the Lake Limnopolar basin in late November 2008, representing peak snow accumulation at the site (Figs 1 & 2). At this time, snowpack in the catchment usually exhibits large spatial variability and terrain characteristics exert a strong control on its distribution. At each measurement location, five snow depth measurements were taken as four points in a 2 m plus pattern from a centre point. Each snow depth was measured to the nearest cm using an aluminium depth probe with the global positioning system (GPS) location (in UTM co-ordinates with elevation) recorded at the centre point. Replicates were taken to negate the effect of local anomalies related to microtopography, stones, or the erroneous perception of reaching the ground surface when encountering a frozen layer. The final depths were obtained by averaging the five measurements, while rejecting the individual measurements with a bias greater than 25% compared to the other four (e.g. López-Moreno *et al.* 2011). A random sampling strategy was adopted to obtain a large number of measurements avoiding sectors with difficult access due to topography and to provide greater flexibility in handling the heterogeneity of the snowpack.

Snow pits were dug at five locations across the watershed. At each snow pit, density was measured in 10 cm intervals using a 1 litre wedge cutter. Each density sample was weighed after extraction. For a particular 10 cm interval, a minimum of two samples were taken. If the difference in mass of the second sample was more than 10 g (or a density of 10 kg m⁻³) compared to the first sample, a third and possibly a fourth sample was extracted. Snowpack temperature was measured to the nearest 0.5°C at the same

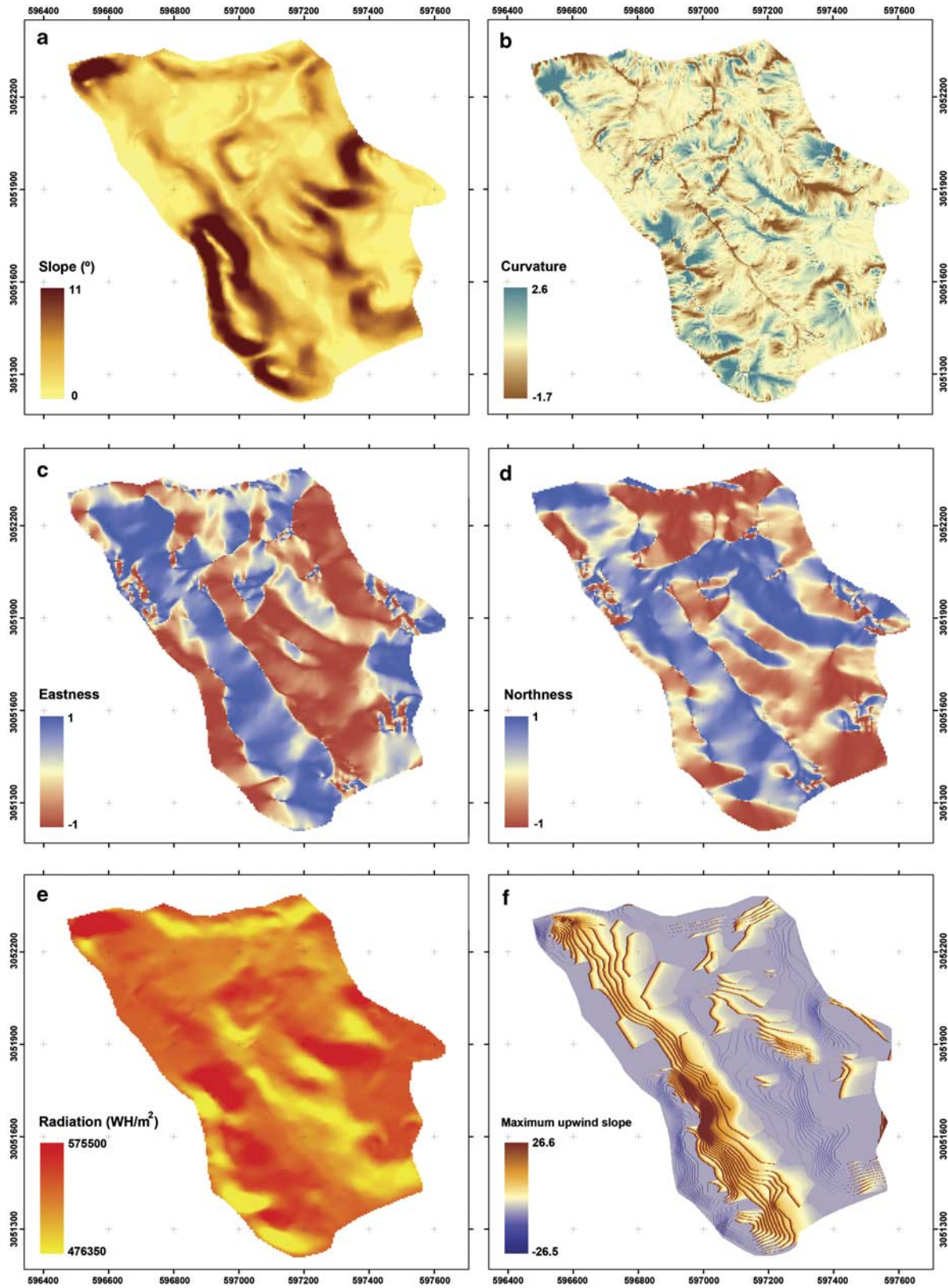


Fig. 2. The distribution of key topographic variables that will be used as surrogates for the meteorology driving the distribution of snow across the Lake Limnopolar watershed. **a.** Slope, **b.** easting, **c.** northing, **d.** curvature, **e.** relative solar radiation, and **f.** maximum upwind slope.

10 cm interval using a dial-stem thermometer. Different snowpack layers were identified visually and manually from changes in hardness. For each layer the snow grain shape (fresh, rounded, sintered, faceted or ice layer) and average grain size was recorded.

Digital elevation model

A digital elevation model (DEM, Fig. 1) was created primarily by transect data collected in 2006 across the study area using a total station. These data were supplemented by three additional sets of points collected with GPS units: a sequence of points along the boundary between the snow-covered (C) and snow-free (F) areas, points at high elevations within the F areas including along the watershed divide, and points at the centre of the snow depth measurements. For the last set of points, the GPS elevation was lowered by the snow depth. It should be noted that the stated GPS horizontal accuracy was 3–4 m, which is good for non-survey grade units. While the absolute error in the elevation is unknown, the relative error is assumed to be small. Also, the points collected with the GPS units were examined and all anomalous elevations, compared to the total survey station data, were removed. The DEM was derived on a 2 x 2 m grid size using the triangulated irregular network (TIN) interpolation procedure available in the ArcGIS 10.0 software package.

Topographic variables

Terrain parameters used as predictor variables of C and F areas were subsequently derived from the DEM.

The selection of potential predictors was based on their ability to affect the rain/snow limit, the motion of fresh snow (i.e. wind drift), and snow ablation. The selected independent variables were:

a) Elevation (Fig. 1), which determines the type of precipitation (solid or liquid) and the evolution of melting in a given area (Caine 1975, Balk & Elder 2000). At the local scale investigated here there is a limited elevational gradient (Fig. 1) and elevation is probably a surrogate for redistribution and snowmelt energetics.

b) Slope (Fig. 2a), which is recognized to affect snow redistribution processes (Mittaz *et al.* 2002).

c) and d) Geographic location given as eastness and northness (Fig. 2b & c), informed on the east–west and north–south orientations of the slopes, respectively. These variables were quantified via the sines and cosines of the aspect, respectively, in a procedure that converted the linear units of the aspects (from 1–360) to circular units (from 1 to -1). Both variables, which logically have collinearity with potential incoming solar radiation, were introduced as predictors because they potentially reflect the effects of snowdrift or deposition by wind (López-Moreno *et al.* 2010).

e) Mean curvature (Fig. 2d), which was used to identify concave and convex areas of the catchment. Landscape curvature, defined as the derivative of the rate of change of the landscape, helps to quantify the shape of the landscape surface. Mean (or overall) curvature is a combination of profile and planiform curvature, and is useful for determining local high and low points. This parameter may play an important role in snowdrift or the deposition of

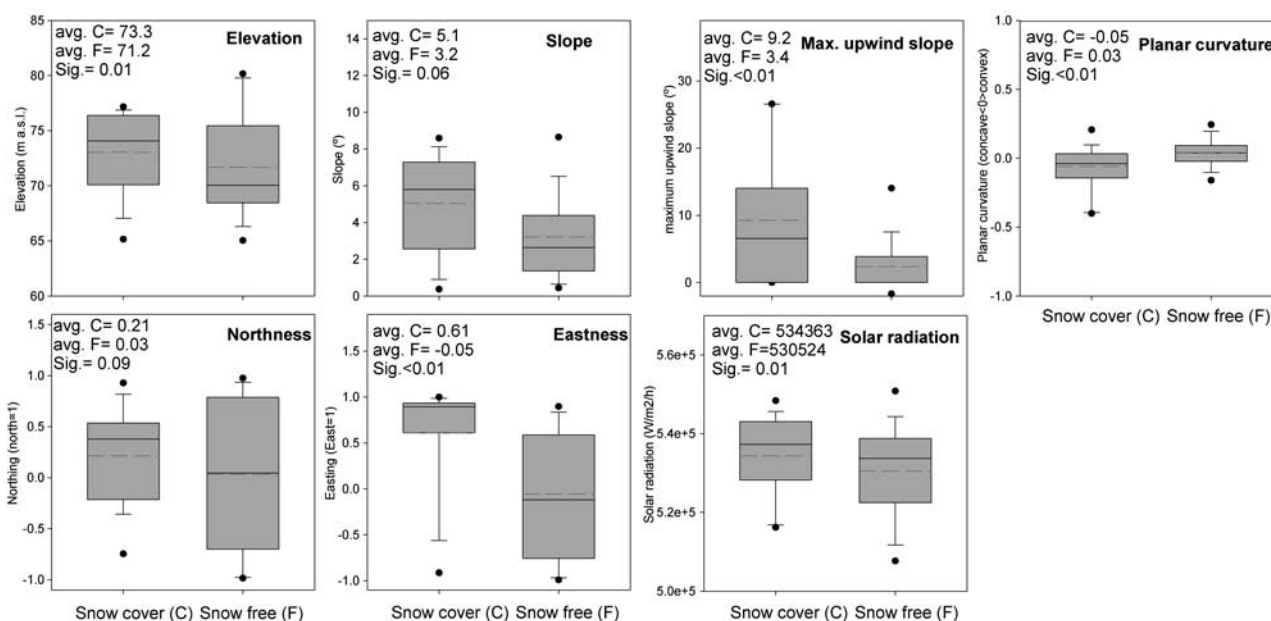


Fig. 3. Box plots of the topographic characteristics found in snow-covered (C) areas and snow-free (F) areas, including the average values for C and F areas plus the statistical significance of the difference between samples based on the Mann-Whitney test for the variables presented in Fig. 1.

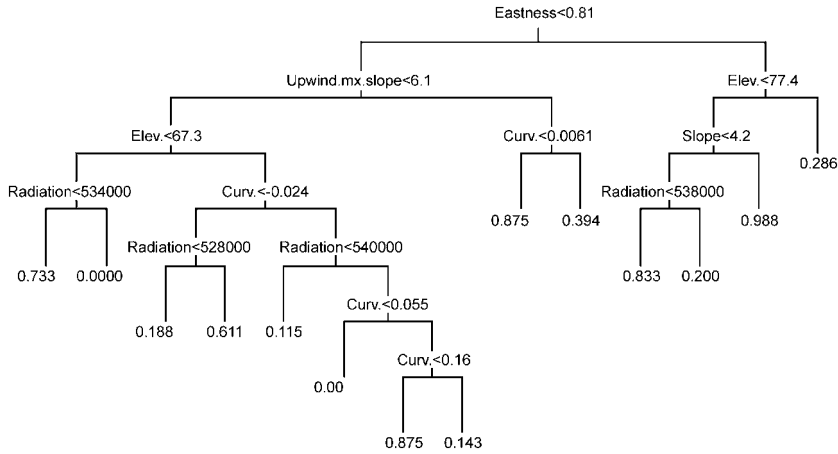


Fig. 4. The regression tree for determining the fractional probability of snow cover.

fresh snow by wind, as well as introducing local modifications into the distribution of incoming solar radiation (López-Moreno *et al.* 2010).

f) Average solar radiation (RAD as Fig. 2e), received by each cell of the DEM from April–November under clear-sky conditions. This parameter was obtained from a physically based computational model (implemented in the MIRAMON GIS software) that considers the effects of terrain complexity (shadowing and reflection), including slope angle and aspect variables. A detailed description of the model can be found in Pons & Ninyerola (2008). Typically the radiation data are presented in watt-hours per square metre ($Wh\ m^{-2}$). However, while many snow distribution studies in alpine areas use clear-sky radiation, the study site is dominated by cloud cover, and since the amount of cloud cover was not included, solar radiation was reported from maximum to minimum as

cloud cover only scales the computed amount. This is further justified since the study basin is small and the solar radiation blockage can be assumed to be uniform across the entire basin.

g) Maximum upwind slope (Winstral *et al.* 2002), which was used to quantify the extent of shelter or exposure provided by the terrain upwind of each pixel on the prevailing wind direction (Fig. 2f). For this study, it was calculated for an azimuth of 260, determined from a wind rose compiled for the Limnopolar meteorological station (Fassnacht *et al.* 2010).

Data analyses

For a first attempt to elucidate the topographic control on the spatial distribution of C and F areas, we compared the

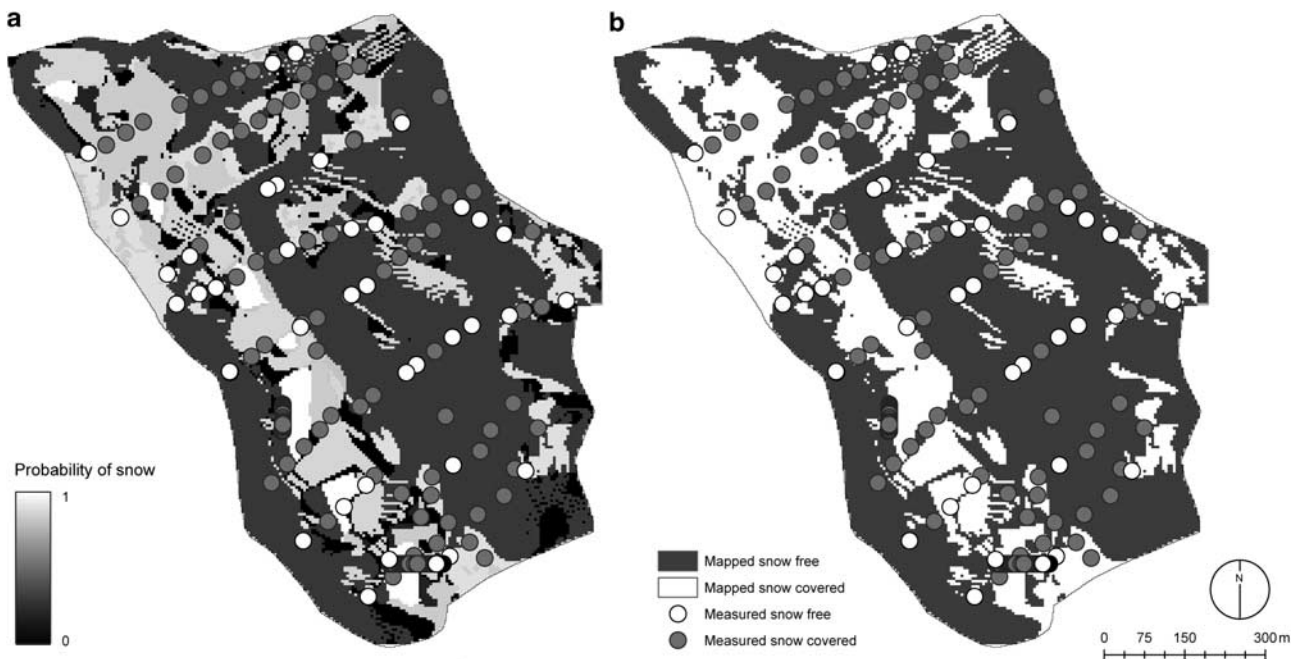


Fig. 5. Map of the basin illustrating **a.** the probability of snow cover classification, and **b.** the snow-covered and snow-free areas.

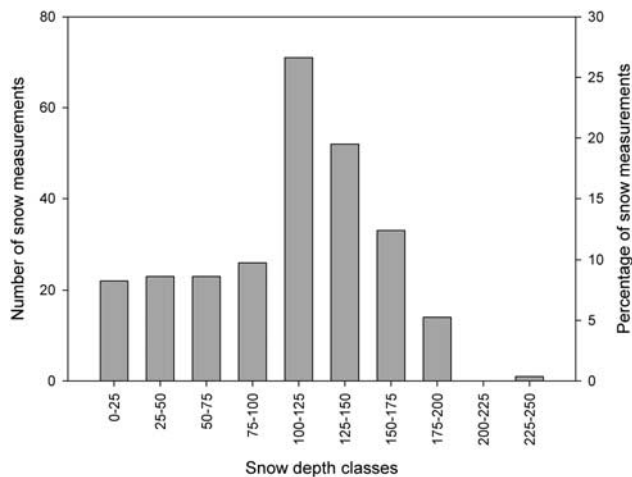


Fig. 6. Histogram of snow depth classes.

topographic characteristics of C and F points sampled during the snow survey (Fig. 3a–g). The existence of statistically significant differences was assessed by means of the Wilcoxon Mann-Whitney test (Siegel & Castelan 1988). Although the Wilcoxon Mann-Whitney test is slightly less powerful than parametric tests such as the *t*-test, it was preferred here because of its robustness against non-normality of the variables (Helsel & Hirsch 1992).

The prediction of C and F areas, and snow depth distribution areas from terrain characteristics were done using regression tree models. Binary regression tree models are non-parametric methods based on the recursive splitting of the information from the predictor variables in order to minimize the sum of the squared residuals obtained in each group (Breiman *et al.* 1984). To apply a regression tree model, the size of the tree must first be selected since fitted trees may be more complex than is warranted by the available data (Anderton *et al.* 2004). An excessive number of nodes hinders the environmental interpretability of data splits. Here, we considered that the inclusion of a new node should contribute to a reduction in unexplained variance by at least 5%. Regression tree models also provide an alternative to the assumption of linearity in relationships between the response variable and the physical characteristics of the terrain (Anderton *et al.* 2004, López-Moreno *et al.* 2006). For modelling

the distribution of C and F areas (Fig. 4), the response variable is binomial (0 and 1, for F and C respectively), and the tree models provide the probability of the existence of snow cover ranging from 0 to 1. In the case of the snow depth (Fig. 5), the response variable, and hence the prediction, are in continuous units (cm of snow depth).

A cross-verification procedure (Guisan & Zimmerman 2000) was used to ensure that verification of the models was done with independent data to that used for model calibration. This technique works by omitting one of the cases, fitting the model to the remainder and then applying the equation obtained to the omitted case in order to calculate its predicted value. This procedure was repeated for all cases in the dataset. Kappa values, *K*, were used to assess the predictive capacity of the model to predict the existence of C and F areas. The Kappa statistic allows the evaluation of model efficacy by assessing the extent to which models predict occurrences that are better than chance occurrences (Fielding & Bell 1997, Manel *et al.* 2001). For example, a Kappa of 0.85 means there is 85% better agreement than by chance alone. Kappa values are drawn from a confusion matrix obtained from the validation dataset. The confusion matrix contains information about observed and predicted snow cover presence or absence through use of a classification system. Kappa values can then be categorized as: predicted and observed; not predicted and not observed; not predicted but observed; and not observed and not predicted classes (Fielding & Bell 1997). Different threshold probabilities to obtain Kappa values (0.1, 0.2, 0.3, 0.4, 0.5, 0.6, 0.7, 0.8 and 0.9) were used in order to obtain a more robust validation and to avoid problems such as prevalence (Forbes 1995). Kappa values vary between 0 and 1. *K* values < 0.4 are considered as being poor, $0.4 < K < 0.75$ are accepted as being good, while *K* values > 0.75 are excellent (Landis & Koch 1997). Observed and predicted snow depths were directly compared and accuracy assessed by the coefficient of determination (r^2), mean bias error (MBE) and mean absolute error (MAE). The two latter were calculated as the average of the difference between the predicted and observed values and the average absolute difference between the predicted and observed values, respectively.

Results and discussion

Almost 30% of the snow measurements were from 100–125 cm in depth, with an almost equal distribution of depths shallower than 100 cm (Fig. 6). However, the difference between the C and the F areas is quite prominent. Most of the topographic variables that dictate the meteorology that drives the presence or absence of snow are significantly different (Fig. 3a–g). Only slope and northness are not significantly different (significance > 0.05) between C and F with eastness, curvature, and maximum upwind slope being considerably different. These differences

Table I. Confusion matrix illustrating the classification capability of the tree model for assigning snow-covered vs snow-free areas over the study watershed. The error of commission is 6% and the error of omission is 22.4%. Overall 88% of the pixels were correctly classified.

		Observed		Total
		Snow-covered	Snow-free	
Predicted	Snow-covered	236	15	251
	Snow-free	35	121	156
	Total	271	136	407

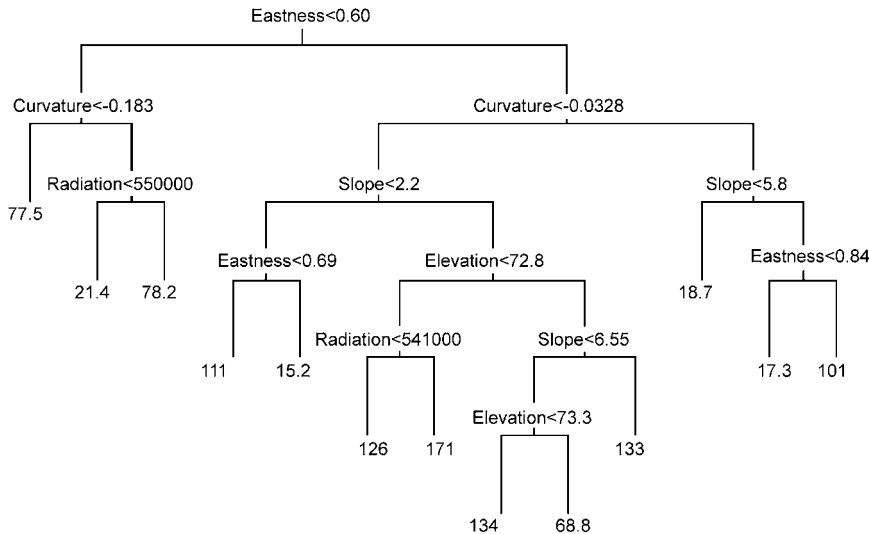


Fig. 7. The regression tree for distributing snow depth (in centimetres).

can also be seen in the regression tree for predicting the probability of snow cover (Fig. 4). Again the variables related to wind effect are those that are more frequent for splitting branches (Fig. 4). The confusion matrix (Table I) highlights how well the regression tree worked. Using a threshold for predicted probability of 0.5 to discriminate C and F classes, 88% of the 407 classes used were properly classified. The errors of omission (predicted as being snow-free but being snow-covered) were 12.9% (35/271) and the errors of commission (predicted as being C but actually being F) were only 6% (15/251). Overall the Kappa score was 0.73, which is considered an excellent score according to the classification suggested by Landis & Koch (1997).

The probability of snow determined by the binary regression tree (Fig. 4) was applied to the topographic variables to yield a map of the probability of snow cover classification (Fig. 5a). The difference between C and F areas was used as the optimum detected threshold, a value of 0.5 to produce the C vs F map (Fig. 5b).

Subsequently for areas with snow cover, the snow depth was determined from a binary regression tree (Fig. 7). Eastness then curvature were the first two variables included. Slope, elevation and solar radiation were also included in the pruned tree. The areas with deeper accumulation are well represented, but the model predicts some snow in areas where it was actually snow-free. This is mostly a consequence of the discrete nature of the tree model predictions, as snow depth is estimated for all the cells of the study area (Figs 7 & 8). In the case of snow cover, the model also predicts the probability of snow cover for all cells (Figs 4 & 5a), but the selection of a threshold of probability (probability > 0.5) to discriminate between C and F areas yields a realistic snow distribution across the study area (Fig. 5, right map).

During the snow survey, areas of snow cover were observed to be contiguous and the banding within the probability of snow map (Fig. 5a) and C vs F map (Fig. 5b) is a result of using a regression tree model and possible artefacts of the DEM generation. These bands can be seen in the maximum upwind slope (Fig. 2f and second node in Fig. 4). This topographic variable is relevant, yet due to the use of the TIN method to interpolate the DEM, slope bands (Fig. 2a) and thus maximum upwind slope bands (Fig. 2f) could have DEM generation artefacts. Other interpolation methods were tested, such as kriging, but they produced less realistic DEMs based on a visual comparison. The original DEM created through the Spanish Polar Programme had some errors of the order of 10m. Therefore the original data used to generate that DEM were individually evaluated and anomalous points were

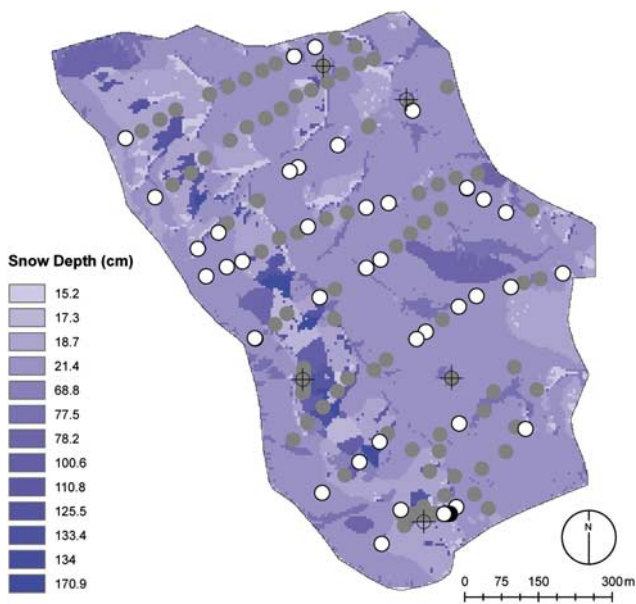


Fig. 8. Map of the distribution of snow depth across the Lake Limnopolar watershed.

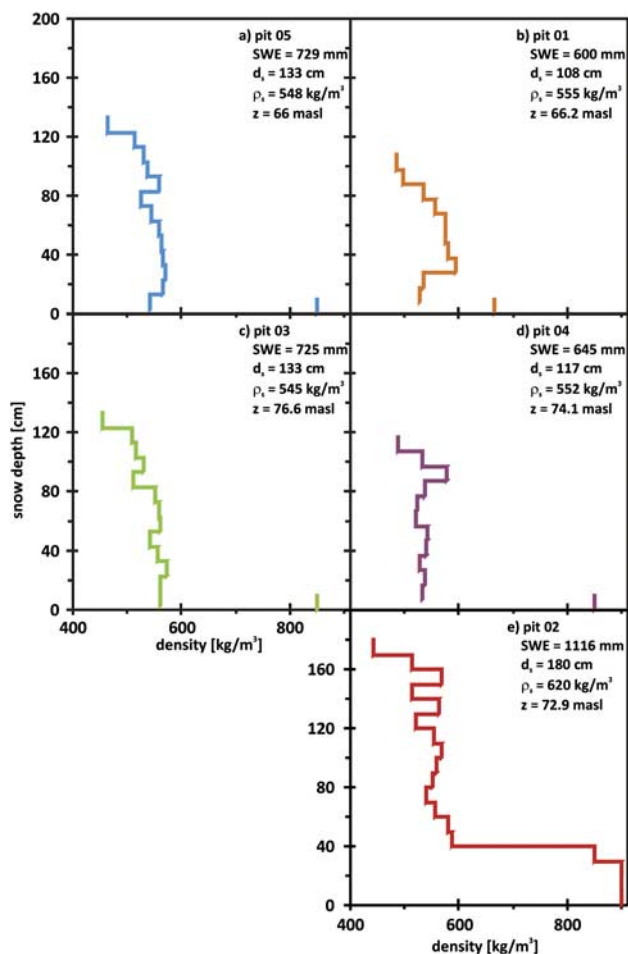


Fig. 9. The variation in snowpack density across the profile and at five locations in the Lake Limnopolar watershed.

removed. It is recommended that the area be resurveyed and DEM generation be evaluated while on-site.

Statistically, the snow depth binary regression tree fit the observed data well with an r^2 value of 0.81 and a mean bias error of only -1.43 cm. The mean absolute error was 21.4 cm. Use of residual interpolation, as per Balk & Elder (2000), would reduce these errors and produce an improved distribution of snow depth. However, the objectives of this paper are to determine the topographic variables controlling the presence/absence of snow and the distribution of the depth of snow rather than to map snow. Due to persistent high winds in these areas, often faster than 15 m s^{-1} (Bañón 2004, Fassnacht *et al.* 2010), the topographic variables associated with wind dictate the presence and distribution of snow.

Snow density profiles were measured at the peak accumulation and/or during the initiation of snowmelt. All snow pits were isothermal to the bottom of the snowpack, i.e. the temperature was 0°C throughout. A basal ice layer was present but its temperature was not measured since equipment was not on hand to access the soil. The five

snow pit density profiles illustrate that the top of the snow is the least dense (450 kg m^{-3}) with some ice layers approaching 600 kg m^{-3} (Fig. 9). For all snow pits, the bottom of the snowpack was much denser. Pits 3, 4 and 5 had an impenetrable basal ice layer of 13, 3, and 3 cm and thus the density of the bottom few centimetres was estimated. Pit 1 had slush at the bottom and pit 2 had standing water at the bottom 30–35 cm. These densities were also estimated. Computing snow density ignoring the bottom ice, slush or water layer yielded an average of 546, 544, 536, 532, and 541 kg m^{-3} for snow pits 1–5 respectively. These averages are all similar, as illustrated in Fig. 9. The denser bottom layers, such as basal ice layers, form primarily due to the presence of permafrost on Byers Peninsula. An active layer forms as the permafrost melts in F areas. The spatial thermodynamics between the F and C areas must be considered when estimating energy within the snowpack and the soil. The proximity and gradient with respect to F areas should be considered when estimating the average snowpack density. The snowpack densities observed herein are at least 100 kg m^{-3} denser than much deeper snowpacks measured in the western United States of America (Mizukami & Perica 2008), probably due to densification by the persistent winds in Maritime Antarctica. At peak snow accumulation it is probably acceptable to assume a mostly homogeneous snow density such as presented by Logan (1973).

The permafrost distribution has been mapped most recently by López-Martínez *et al.* (2012), but it is provided at a scale coarser than snow is mapped in this paper. The distribution of permafrost may influence the distribution of snow, but conversely, the snow distribution does influence the depth of the active layer as deeper snow and later snowmelt hinders the melting of the active layer, i.e. more snow could imply a shallower active layer at the end of the summer. It is possibly that the presence of snow influences the depth of the permafrost.

Conclusions

The presence (snow-covered) or absence (snow-free) of snow at Lake Limnopolar watershed on Byers Peninsula is dominated by topographic variables related to wind. For the binary regression tree, eastness was the first node, with maximum upwind slope, elevation and curvature subsequently dictating the probability of snow. Radiation and slope were also relevant in the model. Neither slope nor northness were statistically different between the snow-covered and snow-free terrain at the 0.05 significance level.

For the distribution of snow depth, eastness was also the dominant variable in the binary regression tree. Curvature, then slope, were next included in the model. Elevation and radiation also appeared. Interpolation of the residuals from the binary regression trees is recommended to produce maps of the distribution of snow depth.

The snowpack density was essentially the same at the five snow pits, when the bottom layers that are influenced by permafrost are disregarded. The total snow water equivalent was different but that is a function of snow depth. Differences in average density across the entire snowpack must consider the proximity and gradient with respect to snow-free areas.

Acknowledgements

Travel to and accommodation in South America was provided by the International Programs at Colorado State University. Travel to Antarctica and logistical support for fieldwork was provided by the Spanish Polar Programme, grant POL2006-06635/CGL from the Education and Culture Ministry (Spain), and from the *Las Palmas* crew (Spanish Navy). Carlos Calvo of the UTM (Maritime Technology Unit, CSIC) and Brendan Keely of the University of York assisted with data collection. Adam Winstral of the Agricultural Research Service in Boise ID provided the code to compute the maximum upwind slope. We would also like to thank two anonymous reviewers for their important insight and their assistance in improving this paper. Thanks are due to Javier Zabalza of the Instituto Pirenaico de Ecología for his assistance with the GIS work.

References

- ANDERTON, S.P., WHITE, S.M. & ALVERA, B. 2004. Evaluation of spatial variability in snow water equivalent for a high mountain catchment. *Hydrological Processes*, **18**, 435–453.
- ANISIMOV, O.A., VAUGHAN, D.G., CALLAGHAN, T.V., FURGAL, C., MARCHANT, H., PROWSE, T.D., VILHJÁLMSSON, H. & WALSH, J.E. 2007. Polar regions (Arctic and Antarctic). In PARRY, M.L., CANZIANI, O.F., PALUTIKOF, J.P., VAN DER LINDEN, P.J. & HANSON, C.E., eds. *Climate change 2007: impacts, adaptation and vulnerability. Contribution of Working Group II to the Fourth Assessment Report of the Intergovernmental Panel on Climate Change*. Cambridge: Cambridge University Press, 653–685.
- BALK, B. & ELDER, K. 2000. Combining binary regression tree and geostatistical methods to estimate snow distribution in a mountain watershed. *Water Resources Research*, **36**, 13–26.
- BAÑÓN, M. 2004. *Introducción al clima de la Península de Byers, Isla de Livingston, Antártida. Comparación con la B.A.E. Juan Carlos I*. MSc thesis, Universidad de Alicante, 112 pp. [Unpublished.]
- BINTANJA, R. 1995. The local surface energy balance of the Ecology Glacier, King George Island, Antarctica: measurements and modelling. *Antarctic Science*, **7**, 315–325.
- BJÖRCK, S., HJORT, C., INGÓLFSSON, Ó., ZALE, R. & ISING, J. 1996. Holocene deglaciation chronology from lake sediments. In LÓPEZ-MARTÍNEZ, J., THOMSON, M.R.A. & THOMSON, J.W., eds. *Geomorphological map of Byers Peninsula, Livingston Island*. BAS GEOMAP series, sheet 5A, 1:25 000, with supplementary text. Cambridge: British Antarctic Survey, 49–51.
- BLÖSCHL, G. 1999. Scaling issues in snow hydrology. *Hydrological Processes*, **13**, 2149–2175.
- BRAUN, M. & HOCK, R. 2004. Spatially distributed surface energy balance and ablation modelling on the ice cap of King George Island (Antarctica). *Global and Planetary Change*, **42**, 45–58.
- BREIMAN, L., FRIEDMAN, J.H., OLSHEN, R.A. & STONE, C.I. 1984. *Classification and regression trees*. Belmont, CA: Wadsworth, 368 pp.
- BRULAND, O., SAND, K. & KILLINGVEIT, Å. 2001. Snow distribution at a high Arctic site at Svalbard. *Nordic Hydrology*, **32**, 1–12.
- CAINE, N. 1975. An elevational control of peak snowpack variability. *Water Resources Bulletin*, **11**, 613–621.
- ELDER, K., DOZIER, J. & MICHAELSEN, J. 1991. Snow accumulation and distribution in an alpine watershed. *Water Resources Research*, **27**, 1541–1552.
- ERICKSON, T.A., WILLIAMS, M.W. & WINSTRAL, A. 2005. Persistence of topographic controls on the spatial distribution of snow in rugged mountain terrain, Colorado, United States. *Water Resources Research*, **41**, 1–17.
- ERXLEBEN, J., ELDER, K. & DAVIS, R. 2002. Comparison of spatial interpolation methods for estimating snow distribution in the Colorado Rocky Mountains. *Hydrological Processes*, **16**, 3627–3649.
- ESSERY, R., LI, L. & POMEROY, J.W. 1999. A distributed model of blowing snow over complex terrain. *Hydrological Processes*, **13**, 2423–2438.
- FASSNACHT, S.R., TORO VELASCO, M., MEIMAN, P.J. & WHITT, Z.C. 2010. The effect of aeolian deposition on the surface roughness of melting snow, Byers Peninsula, Antarctica. *Hydrological Processes*, **24**, 2007–2013.
- FIELDING, A.H. & BELL, J.F. 1997. A review of methods for the assessment of prediction errors in conservation presence/absence models. *Environmental Conservation*, **24**, 38–49.
- FORBES, A.D. 1995. Classification algorithm evaluation: five performance measures based on confusion matrices. *Journal of Clinical Monitoring*, **11**, 189–206.
- GUISAN, A. & ZIMMERMANN, N.E. 2000. Predictive habitat distribution models in ecology. *Ecological Modelling*, **135**, 147–186.
- HELSEL, D.R. & HIRSCH, R.M. 1992. *Statistical methods in water resources*. New York: Elsevier, 522 pp.
- LANDIS, J.R. & KOCH, G.C. 1997. The measurement of observed agreement for categorical data. *Biometrics*, **33**, 159–174.
- LAPEN, D.R. & MARTZ, L.W. 1996. An investigation of the spatial association between snow depth and topography in a prairie agricultural landscape using digital terrain analysis. *Journal of Hydrology*, **184**, 227–298.
- LOGAN, L. 1973. Basin-wide water equivalent estimation from snowpack depth measurements. *Role of snow and ice in hydrology. Proceedings of the WMO/LAHS Symposium, Banff, Alberta, September 1972*. LAHS Publication, No. 107, 864–884.
- LÓPEZ-MARTÍNEZ, J., SERRANO, E., SCHMID, T., MINK, S. & LINÉS, C. 2012. Periglacial processes and landforms in the South Shetland Islands (northern Antarctic Peninsula region). *Geomorphology*, **155–156**, 62–79.
- LÓPEZ-MORENO, J.I. & NOGUÉS-BRAVO, D. 2006. Interpolating snow depth data: a comparison of methods. *Hydrological Processes*, **20**, 2217–2232.
- LÓPEZ-MORENO, J.I., LATRON, J. & LEHMANN, A. 2010. Effects of sample and grid size on the accuracy and stability of regression-based snow interpolation methods. *Hydrological Processes*, **24**, 1914–1928.
- LÓPEZ-MORENO, J.I., FASSNACHT, S.R., BEGUERÍA, S. & LATRON, J.B.P. 2011. Variability of snow depth at the plot scale: implications for mean depth estimation and sampling strategies. *The Cryosphere*, **5**, 617–629.
- LÓPEZ-MORENO, J.I., NOGUÉS-BRAVO, D., CHUECA-CÍA, J. & JULIÁN-ANDRÉS, A. 2006. Glacier development and topographical context. *Earth Surface Processes and Landforms*, **31**, 1585–1594.
- MANEL, S., WILLIA, H.C. & ORMEROD, S.J. 2001. Evaluating presence-absence models in ecology: the need to account for prevalence. *Journal of Applied Ecology*, **38**, 921–931.
- MEIMAN, J.R. 1968. Snow accumulation related to elevation, aspect and forest canopy. *Proceedings of the CNC-IHD Workshop Seminar on Snow Hydrology, Fredericton, February 1968*. Ottawa: Queen's Printer for Canada, 35–47.

- MITTAZ, C., IMHOF, M., HOELZE, M. & HAEBERLI, W. 2002. Snowmelt evolution mapping using an energy balance over an alpine terrain. *Arctic, Antarctic and Alpine Research*, **34**, 274–281.
- MIZUKAMI, N. & PERICA, S. 2008. Spatiotemporal characteristics of snowpack density in the mountainous regions of the western United States. *Journal of Hydrometeorology*, **9**, 1416–1426.
- PONS, X. & NINYEROLA, M. 2008. Mapping a topographic global solar radiation model implemented in a GIS and refined with ground data. *International Journal of Climatology*, **28**, 1821–1834.
- QUESADA, A., CAMACHO, A., ROCHERA, C. & VELÁZQUEZ, D. 2009. Byers Peninsula: a reference site for coastal, terrestrial, and limnetic ecosystem studies in Maritime Antarctica. *Polar Science*, **3**, 181–187.
- RICHARDSON-NÄSLUND, C. 2004. Spatial characteristics of snow accumulation in Dronning Maud Land, Antarctica. *Global and Planetary Change*, **42**, 31–43.
- ROCHERA, C., JUSTEL, A., FERNÁNDEZ-VALIENTE, E., BAÑÓN, M., RICO, E., TORO, M., CAMACHO, A. & QUESADA, A. 2010. Interannual meteorological variability and its effects on a lake from Maritime Antarctica. *Polar Biology*, **33**, 1615–1628.
- SIEGEL, S. & CASTELAN, N.J. 1988. *Nonparametric statistics for the behavioral sciences*. New York: McGraw-Hill, 399 pp.
- THOMSON, M.R.A. & LÓPEZ-MARTÍNEZ, J. 1996. Introduction. In LÓPEZ-MARTÍNEZ, J., THOMSON, M.R.A. & THOMSON, J.W., eds. *Geomorphological map of Byers Peninsula, Livingston Island*. BAS GEOMAP series, sheet 5A, 1:25 000, with supplementary text. Cambridge: British Antarctic Survey, 1–5.
- VAN LIPZIG, N.P.M., KING, J.C., LACHLAN-COPE, T.A. & VAN DEN BROEKE, M.R. 2004. Precipitation, sublimation, and snow drift in the Antarctic Peninsula region from a regional atmospheric model. *Journal of Geophysical Research*, 10.1029/2004JD004701.
- VIHMA, T., MATTILA, O.-P., PIRAZZINI, R. & JOHANSSON, M.M. 2011. Spatial and temporal variability in summer snow pack in Dronning Maud Land, Antarctica. *The Cryosphere*, **5**, 187–201.
- WINSTRAL, A., ELDER, K. & DAVIS, R.E. 2002. Spatial snow modeling of wind-redistributed snow using terrain-based parameters. *Journal of Hydrometeorology*, **3**, 524–538.
- WINSTRAL, A. & MARKS, D. 2002. Simulating wind fields and snow redistribution using terrain-based parameters to model snow accumulation and melt over a semi-arid mountain catchment. *Hydrological Processes*, **16**, 3585–3603.
- WINTHER, J.-G., BRULAND, O., SAND, K., GERLAND, S., MARECHAL, D., IVANOV, B., GLOWACKI, P. & KÖNIG, M. 2003. Snow research in Svalbard - an overview. *Polar Research*, **22**, 125–144.
- WOO, M.-K. 1998. Arctic snow cover information for hydrological investigations at various scales. *Nordic Hydrology*, **29**, 245–266.